

**PHOTOCATALYTIC PERFORMANCE OF g-
C₃N₄/Ag-METAL OXIDES PHOTOCATALYSTS
FOR DEGRADATION OF REACTIVE BLACK 5
(RB5) AND PHENOL UNDER SIMULATED
SOLAR LIGHT**

NOOR IZZATI BT MD. ROSLI

UNIVERSITI SAINS MALAYSIA

2020

**PHOTOCATALYTIC PERFORMANCE OF g-
C₃N₄/Ag-METAL OXIDES PHOTOCATALYSTS
FOR DEGRADATION OF REACTIVE BLACK 5
(RB5) AND PHENOL UNDER SIMULATED
SOLAR LIGHT**

by

NOOR IZZATI BT. MD. ROSLI

**Thesis submitted in fulfillment of the requirements
for the degree of
Doctor of Philosophy**

September 2020

ACKNOWLEDGEMENT

This PhD thesis would not have been possible and completed without the guidance and assistance of several individuals who have spent their valuable time in completing this PhD journey.

Foremost, my sincere gratitude goes to my supervisor, Prof. Dato' Ir. Dr. Abdul Rahman Bin Mohamed for being an outstanding adviser and excellent professor. Secondly, I would like to thank my co-supervisor, Assoc. Prof. ChM. Ts. Dr. Lam Sze Mun for her constant guidance and encouragement. Her thoughtful knowledge was valuable for me so much and without her consistent and long-term patience, it would be hard for me to complete my PhD.

I sincerely thank all the staff and technicians of School of Chemical Engineering for their help given directly or indirectly. Their invaluable help and assistance were always critical for the successful completion of my PhD program. I sincerely thank members from Prof. Abd. Rahman's group for their kindness, friendliness and open-arms to share the knowledge throughout my study. I really appreciate the period we studied together. Special thanks to my friend Rabita, Syahida, Muthmirah, Hayati, Nurul Alia and my roommate Nor Fatehah for always giving support and valuable ideas for me to complete this program.

I am gratefully acknowledging My Brain 15 through Malaysia government and LRGS grant ((No.6720009) for providing me financial support throughout my study. Last but not least, this work is dedicated to my parent Md Rosli Hj Osman and Mek Limah Bt Saoud, whose love, encouragement and moral support have been critical in completing this PhD program. Also, thanks to my brother and sisters for all the support throughout my study.

TABLE OF CONTENTS

ACKNOWLEDGEMENT.....	ii
TABLE OF CONTENTS.....	iii
LIST OF TABLES.....	viii
LIST OF FIGURES.....	x
LIST OF PLATES.....	xiv
LIST OF SYMBOLS	xv
LIST OF ABBREVIATIONS	xvi
LIST OF APPENDICES.....	xvii
ABSTRAK.....	xviii
ABSTRACT.....	xxi
CHAPTER 1 INTRODUCTION.....	1
1.1 Industrial Water Pollution.....	1
1.2 Advanced Oxidation Process (AOP) For Wastewater Treatment.....	4
1.3 Problem Statements	5
1.4 Research Objectives	7
1.5 Scope of Study	8
1.6 Thesis Organization.....	9
CHAPTER 2 LITERATURE REVIEW.....	11
2.1 Environmental Water Pollution.....	11
2.1.1 Reactive black 5 (RB5) as an azo dye.....	13
2.1.2 Phenol	15
2.2 Advanced Oxidation Process (AOP).....	17
2.2.1 Homogeneous and heterogeneous catalysis.....	18

2.2.2	Heterogeneous photocatalysis.....	19
2.3	Mechanism of Heterogeneous Photocatalysis.....	20
2.3.1	Excitation of bandgap energy.....	22
2.3.2	Recombination of electron-hole pairs.....	24
2.3.3	Role of active species.....	25
2.4	Graphitic Carbon Nitride (g-C ₃ N ₄) As A Photocatalyst.....	26
2.4.1	Modification of g-C ₃ N ₄ photocatalyst.....	32
2.4.1 (a)	g-C ₃ N ₄ /single metal oxide.....	32
2.4.1.(b)	g-C ₃ N ₄ /composites oxides.....	35
2.4.1 (c)	g-C ₃ N ₄ /Ag-based photocatalysts.....	39
2.5	Simulated Solar Light As The Light Source.....	45
2.6	Process Variables Study.....	50
2.6.1	Effect of oxidant loading.....	50
2.6.2	Effect of photocatalyst loading.....	52
2.6.3	Effect of initial substrate concentration.....	54
2.6.4	Effect of solution pH.....	57
2.7	Analysis and Identification of Intermediates.....	59
2.8	Kinetic Study.....	63
2.9	Summary.....	66
CHAPTER 3 MATERIALS AND METHODS.....		67
3.1	Materials and Chemicals.....	67
3.2	Equipment.....	70
3.2.1	Stainless steel Teflon-lined autoclave.....	70
3.2.2	Photocatalytic batch reactor.....	71
3.3	Analytical Equipment.....	71
3.3.1	UV-vis spectrophotometer.....	71
3.3.2	High Performance Liquid Chromatography (HPLC).....	73

3.3.3	Total organic carbon (TOC).....	73
3.3.4	Surface charge analysis.....	73
3.4	Preparation of Photocatalyst.....	73
3.4.1	Preparation of g-C ₃ N ₄	73
3.4.2	Preparation of g-C ₃ N ₄ /Ag-metal oxides photocatalysts...	74
3.5	Characterization of Photocatalyst.....	76
3.5.1	Surface morphology.....	76
3.5.2	Crystallinity and phase analysis.....	77
3.5.3	Light absorption analysis.....	77
3.5.4	Surface area measurement.....	78
3.5.5	Electronic structure analysis.....	78
3.5.6	Photoelectrochemical analysis.....	78
3.6	Photocatalytic Test.....	79
3.6.1	Comparison studies for RB5 and phenol degradation.....	80
3.7	Process Parameter Study.....	80
3.7.1	Effect of oxidant loading.....	80
3.7.2	Effect of photocatalyst loading.....	80
3.7.3	Effect of initial substrate concentration.....	81
3.7.4	Effect of solution pH.....	81
3.8	Detection of Reactive Oxidative Species (ROS).....	81
3.8.1	ROS detection.....	81
3.8.2	Hydroxyl radicals (•OH) determination.....	82
3.9	Photocatalyst Reusability.....	82
3.10	Kinetic Studies.....	83
3.11	Electrical Energy Evaluation.....	84

CHAPTER 4	RESULTS AND DISCUSSION.....	86
4.1	Characterization of g-C ₃ N ₄ /Ag-Metal Oxides Photocatalyst For Photocatalytic Reaction.....	86
4.1.1	Crystal structure analysis	87
4.1.2	Surface morphology analysis.....	91
4.1.3	Textural property analysis.....	94
4.1.4	Optical property analysis.....	98
4.2	Photocatalytic Performance of g-C ₃ N ₄ /Ag-Metal Oxides Photocatalysts Under Simulated Solar Irradiation.....	102
4.2.1	Effect of Ag-metal oxides.....	102
4.2.2	Photocatalytic degradation of RB5 at different Ag ₂ Mo ₂ O ₇ loadings.....	104
4.2.3	Comparison study.....	105
4.3	Photocatalytic Mechanism Study for g-C ₃ N ₄ /Ag-Metal Oxides Photocatalysts.....	106
4.3.1	Hydroxyl (•OH) generation.....	106
4.3.2	Reactive oxidative species (ROS) detection.....	108
4.3.3	Photoluminescence (PL) study.....	110
4.3.4	Photoelectrochemical measurement test (EIS).....	111
4.3.5	Proposed photocatalytic mechanism enhancement.....	114
4.4	Process Parameter Study.....	119
4.4.1	Effect of photocatalyst loading.....	119
4.4.2	Effect of initial RB5 concentration	120
4.4.3	Effect of solution pH.....	122
4.5	Photocatalytic Degradation of Phenol Over AMO/BCN Photocatalyst.....	124
4.5.1	Comparison study.....	124
4.5.2	Process parameter studies.....	125
4.5.2 (a)	Effect of oxidant loading.....	127
4.5.2 (b)	Effect of photocatalyst loading.....	129

4.5.2 (c)	Effect of initial phenol concentration.....	129
4.5.2 (d)	Effect of solution pH.....	130
4.6	Photocatalyst Stability Study.....	132
4.7	Mineralization and Reaction Intermediates.....	135
4.7.1	Total organic carbon (TOC).....	135
4.7.2	Intermediates identification.....	136
4.8	Kinetic Studies.....	139
4.8.1	Reaction order.....	139
4.8.2	Langmuir-Hinshelwood kinetic model.....	143
4.9	Electrical Energy Consumption.....	146
4.10	Sunlight photocatalytic activity of AMO/BCN photocatalyst toward degradation of phenol.....	147
CHAPTER 5 CONCLUSIONS AND RECOMMENDATIONS....		149
5.1	Conclusions.....	149
5.2	Recommendations.....	151
REFERENCES.....		152
APPENDICES		
LIST OF PUBLICATION		

LIST OF TABLES

		Page
Table 2.1	Basic physical and chemical properties of phenol (Ahmed <i>et al.</i> , 2010).	16
Table 2.2	Comparative oxidizing power of different oxidants (Mamba and Mishra, 2016; Mousavi <i>et al.</i> , 2018)	18
Table 2.3	Examples of organic contaminants that mineralized by heterogeneous catalysis.	21
Table 2.4	Photocatalytic properties of g-C ₃ N ₄ .	30
Table 2.5	Photocatalytic properties of g-C ₃ N ₄ /single metal oxide.	36
Table 2.6	Photocatalytic properties of g-C ₃ N ₄ /composites oxide.	40
Table 2.7	Photocatalytic properties of g-C ₃ N ₄ /Ag-based photocatalysts.	46
Table 2.8	Effect of oxidants loading to the photocatalyst performance.	53
Table 2.9	Effect of photocatalyst loading to the photocatalytic performance.	55
Table 2.10	Effect of initial substrate concentration to the various photocatalyst.	56
Table 2.11	Effect of solution pH to the various photocatalyst performance.	60
Table 2.12	Representation studies probing the formation of reactive intermediates during phenol degradation.	62
Table 2.13	Reaction kinetic of g-C ₃ N ₄ catalyst system to degrade various pollutants.	65
Table 3.1	List of chemicals and reagents.	69
Table 3.2	Reaction order, kinetic expression, y-axis and x-axis.	83
Table 4.1	Phase structure and average crystallite size of developed photocatalysts.	90

Table 4.2	BET surface area, and pore volume of as-prepare catalysts.	97
Table 4.3	Estimated band gap energy (E_g) of as-prepared photocatalysts	100
Table 4.4	Chemical name and their corresponding retention time.	136
Table 4.5	The values of rate constant (k) and correlation coefficient (R^2) at different reaction rate order for different initial RB5 concentrations under simulated solar light irradiation.	141
Table 4.6	The values of rate constant (k) and correlation coefficient (R^2) at different reaction rate order for different initial phenol concentrations under simulated solar light irradiation.	142
Table 4.7	Comparison study of kinetic degradation between current work and other studies.	144
Table 4.8	Values of k_r and K_{ads} obtained for photodegradation of RB5 and phenol using AMO/BCN photocatalyst.	146
Table 4.9	E_{EO} values obtained for degradation of RB5 and phenol.	147

LIST OF FIGURES

		Page
Figure 1.1	Hazardous pollutants generation by category in the year 2008 (Aja <i>et al.</i> , 2016)	2
Figure 2.1	Growth of fibre production to meet the world population (Kirsi <i>et al.</i> , 2020).	12
Figure 2.2	Molecular structure of Reactive Black 5 (Bilal <i>et al.</i> , 2018).	13
Figure 2.3	Bandgap energy for selected semiconductor photocatalysts (Kumar <i>et al.</i> , 2018).	23
Figure 2.4	Basic principle of photocatalysis. R is chemical that undergoes reduction, O is the chemical that undergoes oxidation process. (I) light harvesting to generate charge carriers; (II and III) separation and transfer of photogenerated charges to the semiconductor surfaces; (III') recombination of photogenerated charges; (IV) surface redox reactions (Zhu and Wang, 2017).	25
Figure 2.5	Basic structure of g-C ₃ N ₄ (Aiwu <i>et al.</i> , 2017)	27
Figure 3.1	Flow chart of experimental work involved in this study.	68
Figure 3.2	Schematic diagram of stainless-steel Teflon-lined autoclave.	70
Figure 3.3	Process flow chart for photocatalyst preparation.	75
Figure 4.1	XRD spectrum for (a) BCN; (b) 20 wt% AMO/BCN; (c) 20 wt% AFO/BCN; and (d) 20 wt% AVO/BCN photocatalysts.	88
Figure 4.2	Narrow angle for g-C ₃ N ₄ and g-C ₃ N ₄ /Ag-metal oxides photocatalyst where (a) BCN; (b) 20 wt% AMO/BCN; (c) 20 wt% AFO/BCN, and (d) 20 wt% AVO/BCN photocatalyst.	89
Figure 4.3	Figure 4.3: XRD pattern of AMO/BCN photocatalyst at different loadings (a) 10 wt%, (b) 20 wt% and (c) 25 wt%.	90

Figure 4.4	FESEM images for (a) BCN; (b) AMO/BCN; (c) AFO/BCN; and (d) AVO/BCN photocatalyst.	92
Figure 4.5	EDX spectra for (a) BCN, (b) AVO/BCN, (c) AFO/BCN, and (d) AMO/BCN photocatalyst.	93
Figure 4.6	N ₂ adsorption-desorption of (a) BCN; (b) AFO/BCN; (c) AMO/BCN and (d) AVO/BCN. The insert figure is the pore distribution of as-prepared photocatalysts.	95
Figure 4.7	Classification of IUPAC isotherm (Cychosz and Thommes, 2018).	96
Figure 4.8	N ₂ adsorption-desorption of AMO/BCN at different weight loadings of 10 wt%, 15 wt%, 20 wt% and 25 wt%.	97
Figure 4.9	(a) UV-vis absorbance spectra and (b) transformation of Kubelka-Munk function of as-prepared photocatalysts.	99
Figure 4.10	(a) UV-vis absorbance spectra for AMO/BCN at different weight loadings; (b) The plot of $[F(R).hv]^{1/2}$ vs $h\nu$.	101
Figure 4.11	The photocatalytic degradation of RB5 over g-C ₃ N ₄ and g-C ₃ N ₄ /Ag-metal oxides photocatalysts.	102
Figure 4.12	Photocatalytic activity of AMO/BCN photocatalyst at different Ag ₂ Mo ₂ O ₇ loadings. (photocatalyst loading = 1 g/L; [RB5] = 10 mg/L; solution pH = 5.1).	104
Figure 4.13	Comparison studies for photocatalytic degradation of RB5. (photocatalyst loading = 1 g/L; [RB5] = 10 mg/L; solution pH = 5.1).	106
Figure 4.14	The TA-PL test for, (a) BCN; (b) AFO/BCN; (c) AVO/BCN and (d) AMO/BCN photocatalysts.	107
Figure 4.15	Photodegradation of RB5 after the addition of scavengers over different g-C ₃ N ₄ /Ag-metal oxides photocatalysts.	109
Figure 4.16	Photoluminescence spectra of g-C ₃ N ₄ and g-C ₃ N ₄ /Ag-metal oxides photocatalysts.	110
Figure 4.17	Photocurrent response of g-C ₃ N ₄ and g-C ₃ N ₄ /Ag-metal oxides photocatalysts.	112

Figure 4.18	The Nyquist plot for g-C ₃ N ₄ /Ag-metal oxides photocatalysts.	113
Figure 4.19	Proposed photocatalytic mechanism for g-C ₃ N ₄ /Ag-metal oxides photocatalysts.	116
Figure 4.20	Effect of photocatalyst loading to the degradation of RB5 using AMO/BCN photocatalyst, ([RB5] = 10 mg/L; solution pH = 5.1)	120
Figure 4.21	Effect of initial RB5 concentration over 20 wt% AMO/BCN photocatalyst, (photocatalyst loading = 1 g/L; pH solution = 5.1).	121
Figure 4.22	Effect of solution pH to photodegradation of RB5 over photocatalyst, (photocatalyst loading = 1 g/L; [RB5] = 10 mg/L).	123
Figure 4.23	Zeta potential versus pH of AMO/BCN photocatalyst.	124
Figure 4.24	Comparison studies for photocatalytic degradation of phenol (photocatalyst loading = 1 g/L; [phenol] = 10 mg/L; solution pH = 5.7).	125
Figure 4.25	(a) Effect of oxidant loading to photodegradation of phenol over AMO/BCN photocatalyst, (photocatalyst loading = 1 g/L; [phenol] = 10 mg/L; solution pH = 5.7); (b) Degradation of phenol over different concentration of NaIO ₄ .	126
Figure 4.26	Effect of photocatalyst loading to photodegradation of phenol over AMO/BCN photocatalyst, ([oxidant] = 106.5 mg/L; [phenol] = 10 mg/L; solution pH = 5.7).	128
Figure 4.27	Effect of initial phenol concentration photocatalytic performance over AMO/BCN photocatalyst, ([oxidant] = 106.5 mg/L; photocatalyst loading = 1 g/L; solution pH = 5.7).	129
Figure 4.28	Effect of pH to the photocatalytic performance of over AMO/BCN photocatalyst, ([oxidant] = 106.5 mg/L; photocatalyst loading = 1 g/L; [phenol] = 5 mg/L).	131
Figure 4.29	Stability test for AMO/BCN photocatalyst for degradation of (a) RB5 ([AMO/BCN] = 1 g/L, [RB5] = 10 mg/L, pH 3) for 30 min; and (b) phenol ([oxidant] = 106.5 mg/L, [AMO/BCN] = 1 g/L, [phenol] = 5 mg/L, pH 5.7) for 70 min	132

Figure 4.30	(a) Fresh AMO/BCN photocatalyst; (b) Spent AMO/BCN photocatalyst.	133
Figure 4.31	XRD result of (a) fresh and (b) spent AMO/BCN photocatalyst.	134
Figure 4.32	Photocatalytic removal and total organic carbon (TOC) analysis of RB5 (1.0 g/L; [RB5] = 10 mg/L and solution pH 3) and phenol ([oxidant] = 106.5 mg/L; 1.0 g/L; [phenol] = 5 mg/L and solution pH 5.7) over AMO/BCN photocatalyst.	135
Figure 4.33	HPLC profile for phenol degradation at different reaction time; (a) 0 min; (b) 10 min; (c) 20 min; (d) 40 min; (e) 60 min and (f) 70 min.	137
Figure 4.34	Proposed degradation pathway of phenol.	138
Figure 4.35	Linearization of L-H model for (a) degradation of RB5 and (b) phenol.	145
Figure 4.36	Photocatalytic degradation of phenol under sunlight (reaction time = 20 min) and simulated solar light irradiation (reaction time = 240 min) over different photocatalysts. ([phenol] = 5 mg/L; photocatalyst loading= 1.0 g/L; pH = 5.7).	148

LIST OF PLATES

		Page
Plate 3.1	Stainless steel Teflon-lined autoclave	70
Plate 3.2	Experimental set up	71

LIST OF SYMBOLS

		Unit
C	Concentration at time t	mg/L
C_0	Initial concentration	mg/L
CO_2	Carbon dioxide	-
e^-	Electron	-
E_g	Bandgap energy	eV
h^+	Holes	-
h	Planck's constant	eVs
HO_2^\bullet	Hydroxyperoxyl radical	-
$h\nu$	Photon energy	-
K	Adsorption equilibrium constant	L/mg
k_{app}	Apparent rate constant	min^{-1}
k_r	Reaction rate constant	mg/L/min
$O_2^{\bullet-}$	Superoxide radical anion	-
O_2	Oxygen	-
$\bullet OH$	Hydroxyl radical	-
OH^-	Hydroxyl ion	-
r	Reaction rate	mg/L.min
R^2	Correlation coefficient	-
pzc	Point charge zero	-
λ	Wavelength	nm
H_2O	Water	-
H_2O_2	Hydrogen peroxide	-

LIST OF ABBREVIATIONS

AOP	Advanced oxidation process
BCN	Bulk g-C ₃ N ₄
CB	Conduction band
HCl	Hydrochloric acid
HPLC	High performance liquid chromatography
L-H	Langmuir-Hinshelwood
NaOH	Sodium hydroxide
NHE	Normal hydrogen electrode
PL	Photoluminescence
RB5	Reactive black 5
SEM	Scanning electron microscope
TOC	Total organic carbon
UV	Ultraviolet-visible diffuse reflectance spectra
VB	Valence band
XRD	X-ray diffraction
CB	Conduction band

LIST OF APPENDICES

Appendix A	Dilution of stock solution
Appendix B	Calibration curve for Reactive Black 5
Appendix C	Calibration curve for phenol
Appendix D	Bandgap energy of pure AgFeO ₂
Appendix E	Bandgap energy of pure Ag ₄ V ₂ O ₇ .
Appendix F	Bandgap energy of pure Ag ₂ Mo ₂ O ₇
Appendix G	Mott-Schottky plots of (a) pure g-C ₃ N ₄ ; (b) pure AgFeO ₂ ; (c) pure Ag ₂ Mo ₂ O ₇ and (d) pure Ag ₄ V ₂ O ₇
Appendix H	Standard retention time for hydroquinone.
Appendix I	Standard retention time for muconic acid.
Appendix J	Retention time for NaIO ₄ .

**PRESTASI FOTOPEMANGKINAN FOTOMANGKIN g-C₃N₄/Ag-OKSIDA
LOGAM UNTUK PENGURAIAN REAKTIF HITAM 5 (RB5) DAN FENOL
DI BAWAH SIMULASI CAHAYA SURIA**

ABSTRAK

Pencemaran persekitaran oleh pelbagai bahan cemar boleh memberi kesan negatif kepada persekitaran dan organisma hidup. Satu kelas Proses Pengoksidaan Lanjutan (AOP) yang dipanggil pemfotomangkinan heterogen oleh pemangkin g-C₃N₄ telah menarik minat sejak akhir-akhir ini untuk rawatan air sisa. Walaubagaimanapun, g-C₃N₄ secara sendiri menghadapi kadar penyatuan semula pasangan e^-/h^+ yang tinggi yang boleh mengurangkan aktiviti fotonya. Oleh itu, gandingan g-C₃N₄ dengan semikonduktor yang mempunyai aras tenaga yang berlainan telah dicadangkan di dalam kajian ini. Satu siri fotomangkin g-C₃N₄/Ag-oksida logam (Ag-oksida logam = AgFeO₂, Ag₄V₂O₇ and Ag₂Mo₂O₇) dihasilkan untuk mengkaji penguraian pemfotomangkinan Reaktif Hitam 5 (RB5) dan fenol di bawah simulasi cahaya solar dan sinaran matahari. Fotomangkin yang dihasilkan dilambangkan sebagai fotomangkin BCN, AVO/BCN, AMO/BCN dan AFO/BCN yang masing-masing sepadan dengan g-C₃N₄ tulen, g-C₃N₄/Ag₄V₂O₇, g-C₃N₄/Ag₂Mo₂O₇ and g-C₃N₄/AgFeO₂. Fotomangkin yang terhasil telah dicirikan oleh Pembelauan Sinar-X (XRD), Mikroskop Elektron Pengimbas (SEM), Spectrum UV-vis Pantulan dan Pengukuran Permukaan Luas BET untuk menentukan sifat fizikal, kimia dan optiknya. Penilaian fotopemangkinan mendedahkan bahawa pemangkin g-C₃N₄/Ag-oksida logam menunjukkan aktiviti fotopemangkinan yang tertinggi untuk penguraian RB5. Terutamanya, pemangkin C₃N₄/Ag₂Mo₂O₇ menunjukkan aktiviti fotopemangkinan yang tinggi dengan 97%

penguraian RB5 dapat dicapai, sementara $g\text{-C}_3\text{N}_4/\text{Ag}_4\text{V}_2\text{O}_7$ dan $g\text{-C}_3\text{N}_4/\text{AgFeO}_2$ masing-masing mempamerkan 83% dan 77%. Kajian mekanistik mencadangkan fotopemangkinan yang telah disiapkan mengikut mekanisme skema-Z. Berbanding dengan C_3N_4 tulen, spektra fotoluminasi (PL) $g\text{-C}_3\text{N}_4/\text{Ag}$ -oksida logam menunjukkan penurunan intensiti yang ketara. Terutamanya, pemangkin $\text{C}_3\text{N}_4/\text{Ag}_2\text{Mo}_2\text{O}_7$ menunjukkan intensiti PL yang terendah. Peningkatan aktiviti foto $\text{C}_3\text{N}_4/\text{Ag}_2\text{Mo}_2\text{O}_7$ disebabkan oleh pemisahan cas yang tinggi dan kesesuaian potensi redoks oleh kedua-dua semikonduktor untuk menghasilkan radikal $\bullet\text{OH}$. Implikasi ini telah dibuktikan oleh ujian pemulih radikal dan asid *terephthalic*-PL (TAPL). Keputusan XRD menunjukkan fotopemangkin $g\text{-C}_3\text{N}_4/\text{Ag}$ -oksida logam mempunyai penghabluran yang tinggi. Penemuan SEM mendedahkan bahawa pembentukan struktur 1D bagi pemangkin AMO/BCN dapat memberikan nisbah permukaan kepada isipadu yang tinggi yang berfaedah kepada penguraian pemfotomangkinan. Hasil penyerapan UV-vis menunjukkan penambahan Ag-oksida logam dapat membantu menyerap lebih tenaga cahaya seterusnya meningkatkan keupayaan optiknya. Pelbagai parameter proses telah dikaji, dan keputusan menunjukkan 99% RB5 terurai di bawah beban pemangkin 1.0 g/L, 10 mg/L dan larutan pH 3. Sementara itu, pada 106.5 mg/L pengoksida, beban pemangkin 1.0 g/L, 5 mg/L fenol dan larutan pH 5.7, 98% fenol telah diurai. Kajian mineralisasi menunjukkan pada keadaan terbaik, kedua-dua RB5 dan fenol boleh dimineralisasi. Kajian kinetik menunjukkan bahawa kinetik bagi kedua-dua bahan pencemar ini mematuhi aturan pertama model Langmuir-Hinsheilwood (L-H). Pemangkin AMO/BCN boleh mengurangkan penggunaan tenaga elektrik untuk penguraian RB5 dan fenol berbanding TiO_2 komersial. Aktiviti fotopemangkinan

di bawah cahaya matahari mencadangkan bahawa pemangkin AMO/BCN adalah pemangkin yang aktif di bawah sinaran matahari.

**PHOTOCATALYTIC PERFORMANCE OF g-C₃N₄/Ag-METAL OXIDES
PHOTOCATALYSTS FOR DEGRADATION OF REACTIVE BLACK 5
(RB5) AND PHENOL UNDER SIMULATED SOLAR LIGHT**

ABSTRACT

Environmental pollution by various hazardous contaminants can give a negative effect to the environment and living organisms. A class of Advanced oxidation process (AOP) called heterogeneous photocatalysis by g-C₃N₄ photocatalyst has attracted recent years for wastewater purification. However, g-C₃N₄ alone suffered from high recombination rate of e^-/h^+ pairs which can inhibit its photoactivity. Thus, semiconductor coupling of g-C₃N₄ with a different energy level of semiconductor has been proposed in this study. A series of g-C₃N₄/Ag-metal oxides (Ag-metal oxides = AgFeO₂, Ag₄V₂O₇ and Ag₂Mo₂O₇) photocatalyst was developed to study the photocatalytic degradation of Reactive Black 5 (RB5) and phenol under simulated solar light. The developed photocatalysts were denoted as BCN, AVO/BCN, AMO/BCN and AFO/BCN photocatalysts corresponding to the pure g-C₃N₄, g-C₃N₄/Ag₄V₂O₇, g-C₃N₄/Ag₂Mo₂O₇ and g-C₃N₄/AgFeO₂, respectively. The developed photocatalysts were characterized by X-ray diffraction (XRD), Scanning Electron Microscope (SEM), Diffuse Reflectance Spectra (UV-vis DRS) and BET surface area measurements to determine their physical, chemical and optical properties. Photocatalytic assessment revealed that g-C₃N₄/Ag-metal oxides photocatalyst exhibited high photocatalytic performance for RB5 degradation. Particularly, g-C₃N₄/Ag₂Mo₂O₇ photocatalyst exhibited the highest photocatalytic activity with 97% degradation of RB5 was achieved, while g-

$C_3N_4/Ag_4V_2O_7$ and $g-C_3N_4/AgFeO_2$ photocatalysts exhibited 83% and 77%, respectively. Mechanistic study suggested as-prepared photocatalyst followed a Z-scheme mechanism. Compared to pure $g-C_3N_4$, the photoluminescence (PL) spectra of $g-C_3N_4/Ag$ -metal oxides showed a significant decrease of photoluminescence intensity of charge carriers and a suitability of redox potential of the two semiconductors to produce $\bullet OH$ radicals. This implication as proven by the radical scavengers test and terephthalic-acid (TA-PL) experiments. XRD result showed that $g-C_3N_4/Ag$ -metal oxides photocatalysts exhibited high crystallinity. SEM finding revealed that the formation of 1D structure of AMO/BCN photocatalyst could provide a high surface to volume ratio which were advantages to the photocatalytic activity. UV-vis absorption result showed that the incorporation of Ag-metal oxides can facilitate in absorbing more light energy, hence enhancing the optical properties. Various operational process parameters were studied, and the findings demonstrated that 99% of RB5 was degraded under 1.0 g/L of photocatalyst loading, 10 mg/L of RB5 and pH solution of 3. Meanwhile, at 106.5 mg/L of oxidant 1.0 g/L of photocatalyst loading, 5 mg/L of phenol and pH solution 5.7, 98% of phenol was degraded. Mineralization study showed that both RB5 and phenol can be mineralized under their best condition. The kinetic study demonstrated that degradation of RB5 and phenol followed a Langmuir-Hinshelwood (L-H) first-order kinetic model. The AMO/BCN photocatalyst can reduced the electrical energy consumption for degradation of RB5 and phenol as compared to those of commercial TiO_2 photocatalyst. Sunlight photocatalytic activity suggested that AMO/BCN photocatalyst was an active photocatalyst under sunlight irradiation.

CHAPTER 1

INTRODUCTION

Environmental pollution has become more serious with significant population growth and expansion of industrial activities since the 21st century. Water covers about $\frac{3}{4}$ of the earth's surface and its consumption contributes approximately 60% - 70% of living beings worldwide. The increased human activities and human population have affected the quality of fresh water supply. In particular, the developing countries have a high potential to discharge more polluted water through domestic use and industrial activities.

1.1 Industrial Water Pollution

Environmental pollution has become a major concern, especially for developing countries. Pollutants enter the water system primarily due to human causes or factors. Daily human activities introduce pollutants into rivers and streams, lakes, groundwater aquifers, and oceans. The pollutants eventually affect the groundwater system and poses a threat to human consumption. The hazardous pollutants can be derived from different sources such as agriculture, industrial, health and household. Industrial sector possesses potential serious hazard as most of the industries employ chemicals, while in agriculture sector hazardous pollutants generally been produced through the used of herbicide, pesticide and fertilizer (Abdul Rani, 1995; Bouman *et al.*, 2002). Pharmaceutical products, chemical wastes, and drugs are among pollutants generate from health sectors (Ghasemi and Yusuff, 2016; Massara and Udaeta, 2010). In homes, a few pollutants are generated such as paints, pesticides, flammable solvents, and caustic cleaners (Fauziah and Agamuthu, 2008; Richardson and Kimura, 2017). Figure 1.1 shows generation of

hazardous waste by category for the year 2008. It can be seen that most of the hazardous pollutants are contributed from heavy metals production. According to the Department of Environment, 11% of the river in Malaysia was registered as polluted in 2017 due to the improper wastewater treatment from industries and agriculture (DOE, 2019). The presence of these toxic substances can lead to long-term toxic health effects that are associated with the ingestion of mixtures of these substances in drinking water.

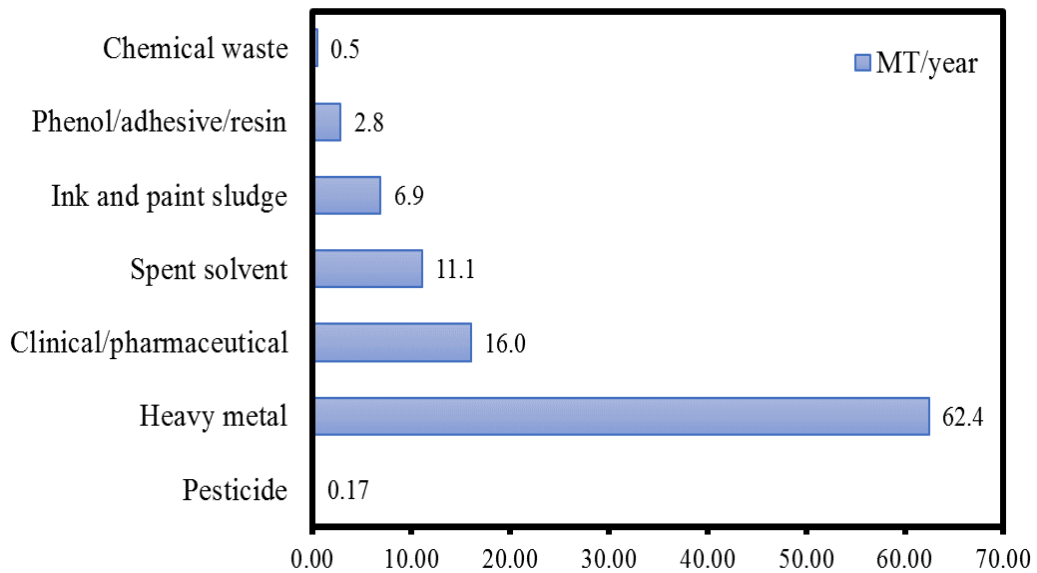


Figure 1.1: Hazardous pollutants generation by category in the year 2008 (Aja *et al.*, 2016).

Dyes and phenolic compounds are among the hazardous pollutants that commonly released to the water bodies. These dye stuffs can cause a threat to the environment due to their low biodegradability in a water system. They are also characterized as chemically stable, non-biodegradable, and carcinogenic. These colourants reduce the penetration of light into the water, and thereby deteriorating

the effectiveness of photosynthesis in aquatic plants. This in turn, causes oxygen depletion and de-regulates the biological cycles of aquatic life.

Phenol and its derivatives are another toxicity and carcinogenicity, which are highly resistant to many processes of degradation including biological and chemical treatments. The presence of phenol may occur naturally in the aquatic environment from the decomposition of aquatic vegetation (Etim *et al.*, 2015). According to United States Environmental Protection Agency (USEPA), phenol is classified as priority of toxic aromatic pollutants (Mojtaba *et al.*, 2018). There are 700 million tons of phenol are generated annually, and it is used as a precursor for numerous products such as herbicides, drugs, paints, lubricants and cosmetics (Senthilvelan *et al.*, 2014; Mohammadi *et al.*, 2015). Wastewater discharge containing phenol and its derivatives can cause severe illnesses, such as leukaemia and some serious organs malfunction may arise when it is overdosed (Mohammadi *et al.*, 2015; Arfin, 2019).

Therefore, it is vital to remove the dye and phenolic compounds from industrial wastewater prior to discharge to the environment. Different traditional wastewater treatments include physicochemical (adsorption, filtration, ion exchange, and osmosis), chemical (ozonation), microbiological (activated sludge, aerobic and anaerobic decompositions), enzyme decomposition and electrochemical often lead to the incomplete mineralization of pollutants. Unfortunately, in many cases, the polluted water was still been found in the river due to less effective treatment being applied by industries. To protect human health and ecosystem, the development of an effective and sustain technique to eliminate organic pollutants is of great importance.

1.2 Advanced Oxidation Process for Wastewater Treatment

Advanced Oxidation Process (AOPs) has emerged as suitable methods for treating a various organic contaminant, including dyestuffs and phenol compounds. AOP is an aqueous phase oxidation technique that produces oxidants with the assistance of photocatalyst, strong oxidants, light or thermal input to destroy the recalcitrant pollutants (Bethi *et al.*, 2016; Du *et al.*, 2018). Example of this methods are Fenton reagents, with or without a source of UV light, photocatalysis, and ozonation have been reported to be useful for the photo-oxidation of organic pollutants (Ngouyap *et al.*, 2010; Hansson *et al.*, 2012; Jing *et al.*, 2015; Du *et al.*, 2018). Among the AOPs techniques, semiconductor heterogeneous photocatalysis has been emerged as a feasible method for destroying various organic and inorganic contaminants into harmless compounds such as CO₂ and H₂O under ambient condition. This technique offers several advantages over other conventional methods, including (Chong *et al.*, 2010; Kumar *et al.*, 2014; Singh *et al.*, 2019) :

- (a) Degrading the pollutants into harmless products with the aid of light irradiation
- (b) Complete mineralization can be achieved.

The semiconductor heterogeneous photocatalysis is known as the acceleration of the photoreaction in the presence of semiconductor photocatalyst and light. The significant application of this process has been applied in wastewater purification and solar water splitting. Following the discovery of water splitting in the presence of TiO₂ by Fujishima and Honda (1972), extensive research has been done to produce hydrogen from water in a reduction-oxidation/redox reaction with various types of semiconductors.

A primary step for the heterogeneous photocatalysis was the absorption of light energy which in return produces the photogenerated electron-holes (e^-/h^+) charges. A series of redox reaction will occur between the photogenerated charges with water, hydroxide ion (OH^-), or oxygen (Ibhadon and Fitzpatrick, 2013). This reaction shortly will form a short-lived intermediate radical like superoxide ($\text{O}_2^{\cdot-}$), hydroxyl ($\cdot\text{OH}$), and hydroperoxyl ($\cdot\text{HO}_2$). These radicals can rapidly attack the organic pollutants and decompose it into harmless substances. Although the lifespan of $\cdot\text{OH}$ is rather short ($\sim 10\mu\text{s}$ in aqueous solution), it is considered as the most powerful oxidizing species, and the first responsible for photodegradation process in aqueous solution (Ismail *et al.*, 2016).

1.3 Problem Statement

Development of industries has generated various types of organic pollutants into the environment. Various pollutants like azo dyes and phenol can give adverse effect to the environment if improper treatment is taken. These substances can cause carcinogenic and mutagenic effect to humans and animals even at low concentrations. The complex structure and recalcitrant in nature of these substances may require an appropriate treatment. To date, heterogeneous photocatalysis has emerged as the wastewater treatment process. Various semiconductors have been explored as the potential photocatalysts such as oxide, sulfide, and oxynitride (Ohno *et al.*, 2014).

In recent years, graphitic carbon nitride ($\text{g-C}_3\text{N}_4$) has become a rising star in the photocatalytic field owing to its low cost, chemically and thermally stable, and most importantly it has a bandgap energy of 2.7 eV which is capable to utilize the visible light (Algara-Siller *et al.*, 2014; Yang *et al.*, 2017). However, the application of $\text{g-C}_3\text{N}_4$ as a photocatalyst is challenging due to its poor response

toward visible light, which makes up about 40% of solar light. The solar light can provide photons with enough energy to excite the photocatalysts as the first step in the cyclic mechanism for the photocatalytic degradation of organic compounds with high efficiency and low costs. Next, the recombination of photoinduced charge carriers for g-C₃N₄ is considered very fast and it suppress the generation of active radicals for photocatalysis reaction. This recombination rate was found to be nearly 10 ns that leads to poor photocatalytic performance (Xiao *et al.*, 2016). Thus, many attempts have been adopted to overcome these limitations including doping with heteroatoms (Raziq *et al.*, 2017; Deng *et al.*, 2017), preparation of nano or porous g-C₃N₄ (Sun *et al.*, 2014; Zhang *et al.*, 2014), and combining with other semiconductors of suitable bandgap and band edge potential (Christoforidis *et al.*, 2016; Han *et al.*, 2014; Pu *et al.*, 2017).

Manipulation of semiconductor band level through combination of different semiconductors is an effective method to suppress the recombination of photogenerated charges carriers. Nowadays, Ag-based photocatalyst has received considerable attention in the photocatalytic field owing to the well-established surface plasmon resonance (SPR) effect can exhibit an excellent visible light-harvesting (Sun *et al.*, 2020). Ag-based semiconductors are responsive in the visible light irradiation owing to their small band gap energy (< 3.0 eV)(Li *et al.*, 2015). Moreover, Ag component can also efficiently promote the separation of photoinduced charge carriers in the photocatalytic process (Fu *et al.*, 2015; Chen *et al.*, 2017). Formation of heterostructure between g-C₃N₄ and a well-matched energy level of Ag-based photocatalyst could tune the electronic properties of g-C₃N₄. Thus, facilitating the mobility of the photogenerated charge carriers for photocatalytic redox process (Ong, 2017).

In developing an efficient g-C₃N₄ coupled catalytic system, the photocatalytic mechanism relating the recombination of photogenerated charges is considered as an important issue (Hao *et al.*, 2016; Liu *et al.*, 2016; Raziq *et al.*, 2017). By far, most of the g-C₃N₄/Ag-based photocatalyst study have shown limited electron and holes mobility between g-C₃N₄ and coupled metal oxides and their basic mechanism on the generation of reactive radical species were scarcely been reported. Thus, the present work is to develop an efficient visible-light g-C₃N₄/Ag-based photocatalyst. The photocatalytic mechanism of g-C₃N₄/Ag-based photocatalyst was studied in the degradation of RB5 and phenol under simulated solar light irradiation. The obtained result also will give insight into the correlation of energy band structures and the successfulness generation of reactive radical species during the photocatalytic reaction.

1.4 Research Objectives

The aim of this research is to develop g-C₃N₄/Ag-metal oxides photocatalyst with a high-performance photocatalytic activity for Reactive Black 5 (RB5) and phenol degradation under simulated solar light irradiation. The specific objectives of this research are:

1. To develop g-C₃N₄/Ag-metal oxides photocatalysts using different metal oxides (Ag- metal oxides = Ag₄V₂O₇, Ag₂Mo₂O₇ and AgFeO₂) via a impregnation-hydrothermal method.
2. To assess the photoactivity of as-synthesized photocatalyst for degradation of RB5 and phenol under simulated solar light irradiation.

3. To study the reaction mechanism and evaluate the the process parameters effects on photocatalytic degradation of RB5 and phenol using the developed photocatalyst.
4. To validate the kinetic process of photodegradation and electrical energy evaluation through the developed photocatalyst.

1.5 Scope of Study

The present study covers the development of photocatalysts, characterization of photocatalyst, photocatalytic performance, mechanistic study of the developed photocatalysts, intermediates determination, kinetic studies as well as electrical evaluation. The dye and phenol concentration were monitored by using UV-vis spectrophotometer and high-performance liquid chromatography (HPLC), respectively. The development of the photocatalyst started with the synthesis of g-C₃N₄ by thermal condensation of its precursor. It was then followed by the addition of Ag-metal oxide photocatalysts such as Ag₄V₂O₇, Ag₂Mo₂O₇ and AgFeO₂ by an impregnation-hydrothermal method. This photocatalysts were chosen because they have a different energy levels that can act as charge separator in g-C₃N₄ systems. The preparation started by mixing an appropriate amount of g-C₃N₄, Ag(NO)₃, (NH₄)₂MoO₄, NH₄VO₃ and Fe(NO₃)₃. The mixture was then transferred into Teflon-lined autoclave and stored in oven at 150°C for 17h. The photocatalytic performance of developed photocatalysts were evaluated on the degradation of Reactive Black 5 (RB5) and phenol as the model pollutants.

The developed photocatalysts were characterized for their physical and chemical properties by field emission scanning electron microscopy (FESEM), energy dispersive X-ray (EDX), X-ray diffraction (XRD), UV-vis absorbance spectra, N₂ adsorption-desorption isotherm, electrochemical analysis, and

photoluminescence spectroscopy. The photocatalytic performance of the as-prepared photocatalysts was assessed by degradation of Reactive black 5 (RB5) and phenol as the model pollutants under simulated solar light irradiation. RB5 and phenol were chosen as the organic pollutant because they were widely spread organic contaminants existed in the wastewater. RB5 is an azo dye which is complex in structure and synthetic in nature, while phenol is a typical intermediate that formed in the degradation of aromatic hydrocarbons. The photocatalytic mechanism of the prepared photocatalyst was studied through the radical scavenger test, photoluminescence terephthalic acid (TA-PL) test and Mott-Schottky test.

The photocatalytic performance of the as-synthesized photocatalysts have been evaluated under different process parameters which include oxidants loading (21.3 – 106.5 mg/L), photocatalyst loadings (0.5 – 2.0 g/L), initial substrate concentration (5 – 40 mg/L, and different pH solutions (pH 3 – pH 10) for the degradation of organic pollutant. These factors were generally reported to have an important influence on the photocatalytic process. Total organic carbon (TOC) have been conducted to evaluate the extent of mineralization of RB5 and phenol. This work subsequently followed by the identification of intermediates in pollutant degradation. The kinetic studies was carried out to determine the reaction order, reaction rate and rate constant of the pollutant degradation processes. Finally, the electrical evaluation was performed on the pollutant degradation process over the developed photocatalyst.

1.6 Thesis Organization

There are five chapters covered in this thesis and each chapter describes the detail of the research study. Chapter 1 (Introduction) provides a general overview of the thesis. This chapter starts with a brief introduction on industrial water

pollution. Then, the advanced oxidation process (AOP) is also described in detail. The chapter also encloses problem statement, research objectives and scope of study. Finally, it is followed by the organization of thesis.

Chapter 2 (Literature review) consists of survey of published literature that has been done on the research topic. The section begins with the background information of dye and phenolic pollutant that leads to this research. Advanced oxidation process, mechanism of heterogeneous photocatalyst, and modification of g-C₃N₄ is then discussed. The process variables and mineralization studies are also covered in this chapter. The kinetic study and electrical energy evaluation is presented in the last section of the thesis.

Chapter 3 (Methodology) describes the detail of material and chemicals used throughout this study. Description of experimental set up, the photocatalyst preparation, photocatalyst characterization, reaction mechanism study, process variable studies, mineralization study, intermediates study, and electrical energy evaluation are presented in this chapter.

Chapter 4 (Result and Discussion) comprises the important research findings gained from this work. This chapter is the main components and it consists of ten sections which includes development of g-C₃N₄/Ag-metal oxides photocatalysts, photocatalytic performance developed photocatalysts, mechanistic study, process variables studies for degradation of RB5 and phenol, photocatalyst stability, mineralization and intermediates identification, kinetic studies, electrical energy consumption and sunlight photocatalytic performance.

Chapter 5 (Conclusions and Recommendations) summarizes all the important findings obtained from this research work. The future recommendations are presented as well.

CHAPTER 2

LITERATURE REVIEW

This chapter provides the literature survey of the semiconductor photocatalysts, including g-C₃N₄ adopted in this area. In Sections 2.1 and 2.2, a brief introduction on the environmental pollution and Advanced oxidation process (AOP) as a promising wastewater treatment were presented, respectively. A basic photocatalysis mechanism of semiconductor and the role of oxidative species involved in photocatalysis were given in Section 2.3. This is followed by a comprehensive review on g-C₃N₄-based as the photocatalyst in the heterogeneous photocatalysis in Section 2.4. An overview on the influence of operational parameters and reactive intermediates on the photocatalytic degradation was discussed in Sections 2.5 and 2.6, respectively. Kinetic studies were discussed in the last Section 2.8.

2.1 Environmental Water Pollution

Water pollution is becoming a serious issue caused by improper treatment of highly toxic organic pollutants from various industries nowadays. Wastewater effluents comes from different sources including factories, laboratories, and domestic sources discharge wastes containing various organic compounds such as pesticide, herbicide, azo dyes and phenol. It has been estimated that azo dye contributed about 80% in the textiles during the dyeing purposes, and approximately 10-15% of the used dyes may be lost through wastewater effluents causing ecotoxic danger (Rajeswari *et al.*, 2017; Sarkar *et al.*, 2017).

According to World Health Organization (WHO), textile industries contributed 17-20% of the water pollution. There are about 280,000 tons of textile

dyes were discharged as the effluents every year worldwide. The substantial increase in clothing consumption has made demand on the textile industries increases per year as shown in Figure 2.1. Global per-capita textile production has shown an increment from 5.9 kg to 13 kg per year from 1975 – 2018 (Kerr and Landry, 2017). Consequently, the long-term effect from this rapid growth of textile industries has led to the increase of water contamination due to dyes.

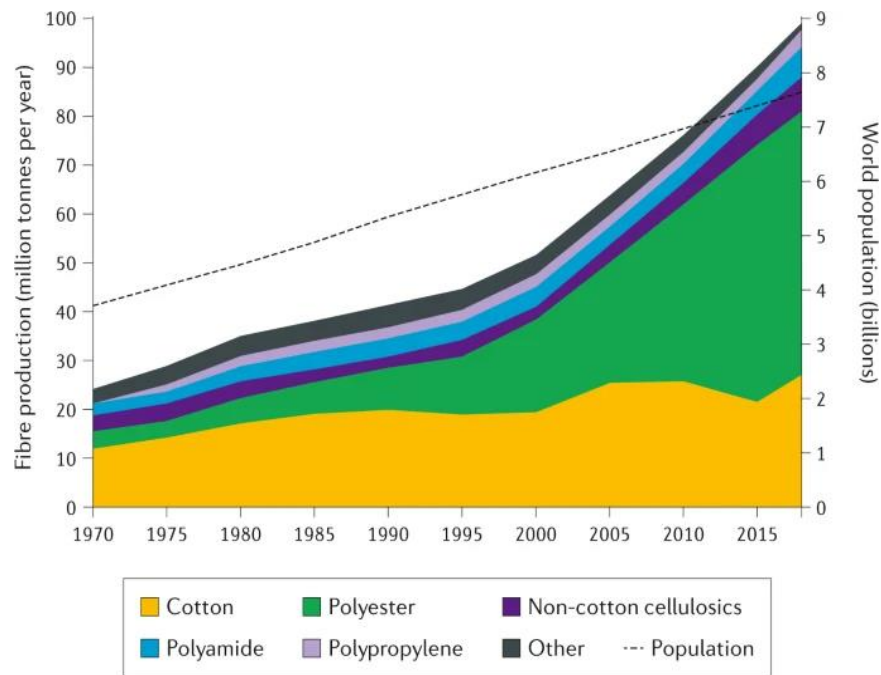


Figure 2.1: Growth of fibre production to meet the world population (Kirsi *et al.*, 2020).

They are various types of dyes that existed in the water effluents such as direct, basic, acid, reactive and azo dyes (Gürses *et al.*, 2016). Azo dyes make up about two third of all synthetic dyes. It is characterized by the chemical formula (R-N=N-R'), where -N=N- shows the presence of azo groups and the R or R' is either aryl or alkyl compound (Chung, 2016). This class of azo dyes constitute to the largest class of synthetic dyes in commercial application (Berradi *et al.* 2019;

Hunger *et al.*, 2000; Lipskikh *et al.* 2018). It was found that the pure forms of many azo dyes were carcinogenic and mutagenic (Saratale *et al.*, 2011). The degradation of azo dyes under natural environment condition usually resulted in a different structure of aromatic amines which in turn they can also have carcinogenic properties (Armina *et al.*, 2019). A large amount of azo dyes is lost during dyeing process, resulting in azo dye containing effluents. Due to their complex chemical structure, azo dyes are resistant to biological activity, ozone, and light (Aracagök and Cihangir, 2013). On the other hand, the physical-chemical treatment is also not destructive, hence a complete removal can not be achieved (Suryawan *et al.*, 2018).

2.1.1 Reactive black 5 (RB5) as an azo dye

Textile dye consist a significant amount of azo dye that are toxic to the environment and aquatic life. Reactive Black 5 (RB5), is widely used reactive azo dyes in textile industry for dyeing cotton and other cellulosic fibres, wool, and nylon. It is also been used in various industries like plastics, photographic, paper, and cosmetics (Dharmar *et al.*, 2018). It consists of two azo groups ($R_1-N=N-R_2$) of the chromophoric components substituted by functional sulfonate ($-SO_3$) and hydroxyl groups ($-OH$). Figure 2.2 shows the molecular structure of RB5.

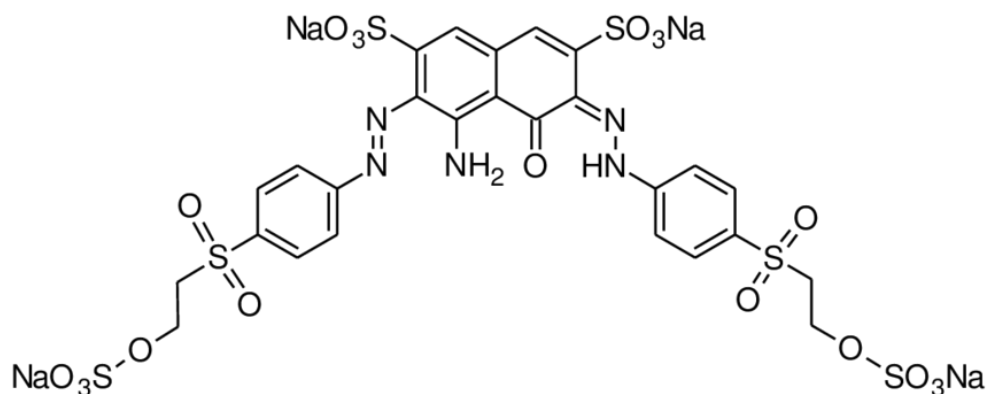


Figure 2.2: Molecular structure of Reactive Black 5 (Bilal *et al.*, 2018).

Reactive azo dyes are very soluble in water and it has a tendency to develop a covalent linkage with –OH, –NH or –SH groups in the textile fibres. Complex chemical structure of these dyes makes it recalcitrant due to its polyaromatic (Fan *et al.*, 2009). Due to the colorant strength, obvious colour changes can be seen even at lower concentration (< 1 ppm) (Ajmal *et al.*, 2014). Compared to the dye molecule itself, their formed intermediates are toxic to aquatic life and mutagenic to human. For example, a study by Gottlieb *et al.* (2003) showed an increase of the toxicity level after degradation with bacteria which reflected to the presence of the aromatic amine and vinyl sulphone.

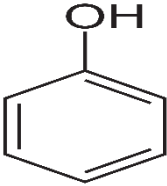
RB5 is highly soluble and recalcitrant in nature owing to its complex chemical structure. The production of aromatic amines during the degradation of RB5 with azo bonds make it highly carcinogenic (Vilar *et al.*, 2011), while it also can be considered as toxic, and mutagenic to various aquatic species (Vedrenne *et al.*, 2012). A study by Dharmar *et al.* (2018) have shown that the presence of RB5 in water caused a severe abnormality, altered the survival and hatching success of zebrafish embryos. This study revealed that the induction of toxicity by the textile dye RB5 to environment. Additionally, the presence of colored effluent can also to the phenomenon known as eutrophication where the water stream lack of oxygen, suffers from algal bloom and results in the death of aquatic life. When this condition happens, less light will penetrate to the river causing the efficiency of the photosynthesis process to reduce. Hence, the amount of oxygen becomes lesser and aquatic life will die (Hadibarata *et al.*, 2013). Environmental Quality Act 1974 has limit that the discharge condition for colour effluent is 100 ADMI and 200 ADMI for Standard A and Standard B, respectively based on the American Dye Manufacturers Institute (ADMI) (Environmental Department, 2019).

2.1.2 Phenol

Phenol belongs to a monosubstituted aromatic compound with a –OH group is attached directly to a benzene ring. Other common names for phenol are hydroxybenzene, benzenol, monophenol, phenyl alcohol and phenyl hydroxide. At the room temperature phenol exists as a colourless, crystalline mass, white powder or syrup liquid when mixed with water (Mohammadi *et al.*, 2015). Phenol is commonly been produced from industries, like chemical, pharmaceutical, textile, paint, oil refinery, and agriculture (Mojtaba *et al.*, 2018). Industrial usage of phenol is widespread since it is been used as an intermediate's chemical. The application of phenol in daily life include wood products, paint and coatings, and cleaning and furnishing care products. Phenol possesses a serious threat to various creatures and human beings. At high concentration (100 - 1000 μ g/L), they can cause unpleasant of taste and odour, and leads to carcinogenic problem (Gami, 2014). Table 2.1 shows the physical and chemical properties for phenol.

The production and use of phenols from the chemical industries can be released into the environment by mainstream. The release of phenol also occurs during the disposal of industrial wastes such as refineries (6-500 mg/L), coking operations (28-3900 mg/L), coal processing (9-6800 mg/L), and the manufacture of petrochemicals (2.0-1220 mg/L) (Mohammadi *et al.*, 2015). Due to its toxicity, it was reported that phenol is placed in the priority list of highly hazardous chemicals (Senthilvelan *et al.*, 2014). Environmental Protection Agency (EPA) has regulated the discharge limit of phenol into water stream should not exceed 2 mg/L (Mojtaba *et al.*, 2018). According to Malaysia's Environmental Law, the discharge limit for industrial effluents must meet the standard as recorded in Fifth Schedule, Environmental Quality (Industrial Effluent) Regulations 2009. Hence, the

Table 2.1: Basic physical and chemical properties of phenol (Ahmed *et al.*, 2010).

Structural formula	
Empirical formula	C ₆ H ₅ OH
Molecular weight (g/mol)	94.11
Color/form	Colorless to white solid
Odor	Slight odor
Melting point (°C)	40.91
Boiling point (°C)	181.75
Water solubility, g/L at 25 (°C)	8
Acidity in water (pK _a)	9.89
Flash point (°C)	79

discharge limit for phenol is 0.001 mg/L and 1 mg/L for Standard A and Standard B, respectively (Environmental Quality Act 1974).

Phenol is soluble in water, oil, carbon disulphide, and most organic solvents like alcohols, ethers, and ketones. The presence of phenol in wastewater can also lead to the formation of substituted compounds during disinfection and oxidation process (Mohammadi *et al.*, 2015). Phenol is a highly corrosive chemical and can give short-term effect and long-term effects on human. Inhalation or ingestion of phenol during contact can cause skin and eyes burning (ATSDR, 2014).

Absorption of phenol onto the skin can facilitates the transfer of phenol to the gastrointestinal tract. At this condition, phenol undergoes metabolism and produce various reactive intermediates form, resulting in their ability to posseses thread to humans (Schweigert *et al.*, 2001). Contaminated drinking water by high concentration of phenol resulted in gastrointestinal tract and muscle tremor with

difficulty in walking (Anku *et al.*, 2017). The presence of phenol in water can also lead to the formation of substituted compounds during the oxidation and disinfectant process. Furthermore, this chemical can perform an inhibitory effect on microorganism in the biological treatment process, and are regarded as secondary pollutants (Rappoport, 2003).

2.2 Advanced Oxidation Process (AOP)

In an effort to find an effective and low-cost technology for wastewater treatment, Advanced Oxidation Process (AOP) has emerged as an innovative technology for wastewater treatment. AOP usually comprises the use of strong oxidizing agents like hydrogen peroxide (H_2O_2) or ozone (O_3), catalysts (iron ions, metal oxides), and irradiation (UV light, solar, ultrasounds) separately or in combination under room temperature and pressure. So far, light driven AOPs is an attractive method for wastewater treatment because of the abundance of solar light and comparatively low costs. The rationales of AOPs are based on the formation of reactive oxidative species like $\bullet\text{OH}$ radicals, H_2O_2 , and $\text{O}_2^{\bullet-}$ in the mechanism to mineralize the organic compounds in wastewater. Table 2.2 lists the comparative oxidizing power of different oxidants.

As shown in Table 2.2, the $\bullet\text{OH}$ radicals possess a higher oxidation potential compared to other oxidants. These strong oxidizing species make it capable to degrade a variety of recalcitrant organic pollutants such as pesticides, dyes, aromatic, chlorinated and phenolic compounds (Poyatos *et al.*, 2010; Bethi *et al.*, 2016; Boczkaj and Fernandes, 2017). This radical reacts with the organic pollutants and initiate a series of redox reactions until the pollutants are mineralized into CO_2 , water and harmless products. Compare to other treatment processes, AOPs are

Table 2.2: Comparative oxidizing power of different oxidants (Mamba and Mishra, 2016; Mousavi *et al.*, 2018).

Oxidants	Oxidizing Potential (eV)
Hydroxyl radicals ($\bullet\text{OH}$)	2.80
Ozone (O_3)	2.07
Hydrogen peroxide (H_2O_2)	1.80
Perhydroxyl radical ($\bullet\text{HO}_2$)	1.70
Permanganate ion (MnO_4)	1.70
Chlorine dioxide (ClO_2)	1.50
Chlorine (Cl_2)	1.35
Superoxide radicals ($\bullet\text{O}_2$)	0.90

superior due to the complete mineralization of wastewater organic pollutant.

2.2.1 Homogeneous and heterogeneous catalysis

In chemistry, the catalysis term implies the process of increasing the rate of reaction in the presence of catalyst. Catalytic approach might be considered as the green since the chemical reaction could be achieved in a shorter time, significantly reducing the cost for the raw materials. Catalysts can be divided into two types, homogeneous and heterogeneous catalysts. Homogeneous catalysis is referred to the chemical reaction that occurs in the same phase of reactants, in which the catalyst is dispersed either in an aqueous or gas mixture with the reactants. An example of homogeneous catalysis is acid catalyst (Bánsági and Taylor, 2017; Thoai *et al.*, 2017). The acid dissolved in water to generate a proton that speeds up chemical reaction, like in hydrolysis of esters. The presence of acid can hydrolyze the ester at a faster rate. Nevertheless, separation of homogeneous catalyst from the reaction mixtures is tedious and costly. In some cases, it can be deposited on the reactor wall

and cause corrosion to the industrial materials (Sivaramakrishna *et al.*, 2012; Habibi *et al.*, 2013) .

Conversely, in heterogeneous catalysis reaction the catalyst and the reactant exist in a different phase. For example, the reaction of gases (or liquid) on the surface of solid catalyst (Cole-Hamilton and Tooze, 2006). Generally, the catalytic reaction occurs on the catalyst surface, hence a high surface area of the catalyst could promote the reaction faster. Heterogeneous catalysts are also easier to prepare and separated from the reaction mixture. The catalysts are generally a metal or metal oxides and they tend to give rather unselective catalytic reactions (Ali *et al.*, 2014).

2.2.2 Heterogeneous photocatalysis

Heterogeneous photocatalysis, a class of AOPs has been regarded as a sustainable environmental technology, which can degrade organic contaminants in wastewater with low cost and high efficiency (Shi *et al.*, 2019). This method offers several advantages which include:

- (a) High reactivity under ambient condition.
- (b) Formation of harmless products. A complete mineralization of organic pollutants is converted to CO₂ and water.
- (c) The formation of photocatalysed intermediate stable products is avoided.
- (d) The photocatalytic reaction can be applied to a wide range of organic compounds in wastewater streams.

Generally, heterogeneous photocatalysis in the liquid phase will degrade organic contaminants into corresponding intermediates and further mineralization into carbon dioxide and water can be achieved if the irradiation time is extended

(Chong *et al.*, 2010). The ideal photocatalyst material should exhibit excellent carrier's separation efficiency, high redox potentials, broad light absorption and good stability (Yuanyuan *et al.*, 2019). As being proposed by Chong *et al.* (2010), the overall photocatalysis reaction can be divided into five independent steps which are:

1. Mass transfer of the reactants from the liquid phase to the photocatalyst surface.
2. Adsorption of the reactants onto the photon activated photocatalyst surface.
3. Photocatalysis reaction for the adsorbed phase on the photocatalyst surface.
4. Desorption of the products.
5. Removal of the products from the interface region to the bulk fluid.

Accordingly, a highly active $\bullet\text{OH}$ radicals were generated in step (3) which in turn mineralized the organic contaminants. There are various types of organic pollutants that have been treated in the photocatalytic processes. Dyes, phenolic compound, pesticide are among classes of organic pollutants that can be degraded by AOP. Table 2.3 lists various types of contaminants that are undergoing mineralization by heterogeneous photocatalyst. The non-selective and total mineralization can be achieved using this method are strongly related to the reactive oxidative species as previously described in Section 2.2.

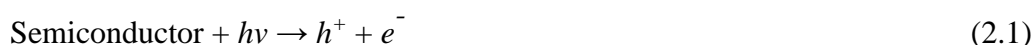
2.3 Mechanism of Heterogeneous Photocatalysis

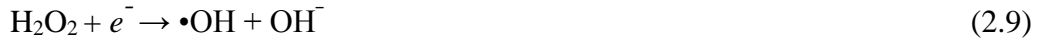
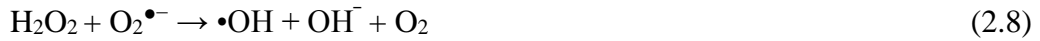
Heterogeneous photocatalysis has been regarded as an efficient method to

Table 2.3: Examples of organic contaminants that mineralized by heterogeneous catalysis.

Class of organics	Examples	References
Dyes	Rhodamine B, methylene blue, methyl orange	Ge <i>et al.</i> (2011), Fu <i>et al.</i> (2014), Fang <i>et al.</i> (2015), Zhu <i>et al.</i> (2015)
Haloaromatics	1,2,4-trichlorobenzene	Zheng <i>et al.</i> (2011)
Halophenol	2-chlorophenol, 4-chlorophenol, 2,4-dichlorophenols	Cui <i>et al.</i> (2012), Chai <i>et al.</i> (2014), Ba-Abbad <i>et al.</i> (2016)
Pesticide	2,4,-dichlorophenoxyacetic acid, 2,4,D-dichlorophenoxypropionic acid, carbendazim, atrazine, malathion	Fouad and Mohamed, (2012), Abdennouri <i>et al.</i> (2016), Bhoi <i>et al.</i> (2018), Khavar <i>et al.</i> (2018)
Phenyl	Phenol, toluene	Yusoff <i>et al.</i> (2014), Sun <i>et al.</i> (2017)
Heavy metals	Cr(VI), Cd ²⁺	Rashed <i>et al.</i> (2017), Mavinakere <i>et al.</i> (2018)

degrade organic contaminants under atmospheric condition. Basically, the role of a photocatalyst is to initiate or accelerate the redox reactions in the presence of light irradiation. Huanli *et al.* (2014) simplified the reaction mechanism into several parts: (i) charge carriers' generation; (ii) charge-carrier trapping; (iii) charge-carrier recombination; and (iv) mineralization of the products. The mechanism of heterogeneous photocatalysis is given in Equations (2.1) - (2.12) (Gholizadeh *et al.*, 2017; Le *et al.*, 2017):





The photoreactions in Equations (2.2) - (2.12) describes the key role of photoexcited charges in the degradation of pollutants. The generated reactive oxidative species like $\text{O}_2^{\bullet-}$, $\bullet\text{OH}$, and $\bullet\text{HO}_2$ underwent a series of chain reaction during the photocatalytic process and subsequently degraded the target pollutants.

2.3.1 Excitation of badgap energy

The redox potential and bandgap energy (E_g) of a photocatalyst are main factors controlling the generation of charge carriers. The bandgap energy (E_g) is defined as the energy difference between the conduction band (CB) and valence band (VB) of a semiconductor. The bandgap energy of the semiconductor largely determines the likelihood and rate of charge transfer, and hence the key design parameters for photocatalysis. Every semiconductor has their corresponding

bandgap energy that will show their photocatalytic activity either in UV light or visible light region. The size of the bandgap energy will determine the optical properties and colour of the photocatalyst. For example, semiconductor ranging from 1.5 eV to 3.0 eV will absorb energy within the visible light range and have colours from red to violet (Mamba and Mishra, 2016). Figure 2.3 shows some selected semiconductors and their respective bandgap energies.

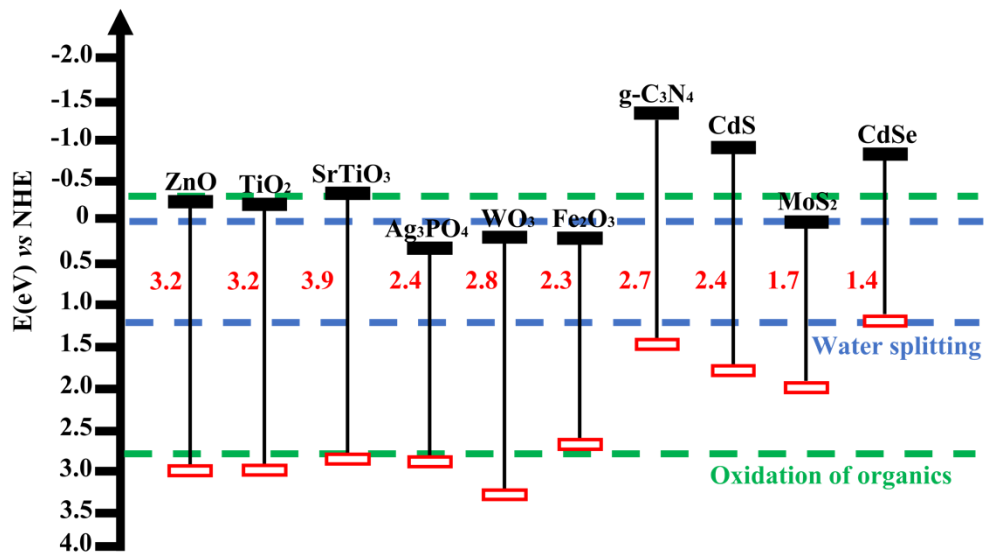


Figure 2.3: Bandgap energy for selected semiconductor photocatalysts (Kumar *et al.*, 2018).

Equation (2.1) indicates that the semiconductor photocatalyst is largely depend on the bandgap energy of the semiconductor. When the semiconductor is irradiated with energy equal to or more than its bandgap energy, an electron-hole ($e^- - h^+$) pairs are produced. The minimum energy that is required by the semiconductors to initiate the photoexcitation are determined using the Equation (2.13) (Pawar *et al.*, 2018):

$$E_g = h\nu \quad (2.13)$$

where h is the Planck's constant ($6.62607 \times 10^{-34} \text{ m}^2 \text{ kg/s}$), and ν is the frequency of incident light. Following the photoexcitation, the electron (e^-) will occupy the CB and leaving positive holes (h^+) in the VB. In order for the occupied e^- to be transferred to the acceptor, the CB of the photocatalyst should be at positive potential as compared to the acceptor's potential. Similarly, the potential level of VB should more negative than the donor in order to accept the h^+ . The photogenerated electron-hole pairs can act as the strong reductant or oxidant to react with electron donors and electron acceptors adsorbed on the catalyst surface.

Figure 2.4 describes the possible steps that are involved once the ($e^- - h^+$) pairs are excited. Reaction (I) is the absorption of light to generate charge carriers. Once excited, the photogenerated charges separated and the photogenerated e^- undergoes reduction process with the target molecule (R), while the oxidation process occurs between the target molecule (O) and the migrating h^+ as described in Reaction (II-IV). However, the photocatalytic performance of the semiconductor depends on the Reaction (III') where the recombination of the photogenerated charges occurs.

2.3.2 Recombination of electron-hole pairs

The recombination of photogenerated charges becomes unfavourable to the photocatalytic efficiency of the photocatalyst. It should be noted that the recombination between the photogenerated charge carriers can occur and dissipate the energy in the form of heat. The recombination can occur either in the volume of the photocatalyst or on the surface of the photocatalyst, with the heat as the by-product. The recombination of the photogenerated charges is considered very fast which is about 10 ns, with 90% of the photogenerated charges will recombine